Published in final edited form as:
Acta Biomater. 2012 November ; 8(11): 4031–4042. doi:10.1016/j.actbio.2012.07.010.

Microstructural and Mechanical Differences Between Digested Collagen-Fibrin Co-Gels and Pure Collagen and Fibrin Gels

Victor K. Lai[1], **Christina R. Frey**[2], **Allan M. Kerandi**[3], **Spencer P. Lake**[2], **Robert T. Tranquillo**[1,2], and **Victor H. Barocas**[*,2]

[1]Department of Chemical Engineering and Materials Science, University of Minnesota – Twin Cities, 421 Washington Ave SE, Minneapolis, MN 55455

[2]Department of Biomedical Engineering, University of Minnesota – Twin Cities, 7-105 Nils Hasselmo Hall, 312 Church Street SE, Minneapolis, MN 55455

[3]Department of Biochemistry, Molecular Biology, and Biophysics, University of Minnesota – Twin Cities, 6-155 Jackson Hall, 321 Church Street SE, Minneapolis, MN 55455

Abstract

Collagen and fibrin are important extra-cellular matrix (ECM) components in the body, providing structural integrity to various tissues. These biopolymers are also common scaffolds used in tissue engineering. This study investigated how co-gelation of collagen and fibrin affected the properties of each individual protein network. Collagen-fibrin co-gels were cast and subsequently digested using either plasmin or collagenase; the microstructure and mechanical behavior of the resulting networks were then compared with respective pure collagen or fibrin gels of the same protein concentration. The morphologies of the collagen networks were further analyzed via 3-D network reconstruction from confocal image z-stacks. Both collagen and fibrin exhibited a decrease in mean fiber diameter when formed in the co-gels compared to the pure gels; this microstructural change was accompanied by increased failure strain and decreased tangent modulus for both collagen and fibrin following selected digestion of the co-gels. In addition, analysis of the reconstructed collagen networks indicated presence of very long fibers and clustering of fibrils, resulting in very high connectivities for collagen networks formed in co-gels.

Keywords

collagen; fibrin; microstructure; mechanical properties; confocal microscopy; tissue engineering

INTRODUCTION

Naturally occurring biopolymers such as collagen and fibrin play an important role in the physiological and mechanical function of various systems and processes in the human body. Collagen, the most abundant protein in the human body, is divided into many different types that are structurally distinct from one another, with type I being most prevalent [1]. Fibrin is

[*]**Corresponding Author:** Victor H. Barocas, 7-105 Nils Hasselmo Hall, 312 Church Street SE, Minneapolis, MN 55455, Ph: 612-626-5572, Fx: 612-624-6583, baroc001@umn.edu.

the main matrix component found in a blood clot and early granular tissue during the wound healing process. These extracellular matrix (ECM) components are also commonly used as scaffolds for tissue engineering applications, including in combination with one another or other proteins, e.g. collagen-fibrin [2], collagen-elastin [3]. Understanding how various ECM components interact with each other to confer overall mechanical behavior is important in more rational design in tissue engineering. The choice of initial scaffold material(s) for seeding cells is a critical aspect in fabricating tissues with structural integrity and biochemical functionality akin to those of native tissues because cells respond differently according to their mechanical and biochemical environments. For example, our group has found that seeding vascular smooth muscle cells (SMCs) in a fibrin gel promotes cellular production of collagen I, hence improving the mechanical strength of the overall tissue equivalent (TE) [4]. Regardless of the initial choice of scaffold material, engineered tissues, like native tissues, almost always contain a combination of different ECM components. For example, compositional changes in the ECM occur in fibrin-based constructs during the growth and remodeling process where the fibrin matrix is gradually degraded and replaced by a cell-derived collagen matrix [5–7], a process akin to wound healing. While the structure and mechanics of individual ECM components (e.g. collagen, fibrin, elastin) have been studied extensively [8–16], understanding of composite ECM systems is still lacking. Previous studies on interpenetrating network systems, both in synthetic polymer blends [17,18] and natural biopolymer [19–21] mixtures, have shown complex mechanical responses, indicating complex interactions between the networks that are not well understood.

Specifically for collagen-fibrin co-gels, previous studies on interactions between these two ECM components have reported conflicting results, with some [22,23] refuting the presence of chemical bonding between these proteins as reported in [24]. Our group is interested in understanding how network architectures and interactions in interpenetrating ECM systems influence overall mechanics and in developing a computational model that can adequately capture the mechanics of such systems based on their respective microstructural and mechanical details. That network morphology and mechanical behavior of *individual* collagen and fibrin networks can be altered by varying gelation conditions has been well documented. For fibrin, seminal studies by Ferry and co-workers investigated effects of fibrinogen and thrombin concentrations as well as pH, temperature and ionic strength of the solutions [25]; this work was followed by similar studies conducted by other groups, (e.g. [26–30]). More recent work by our group [31] and others (e.g. [32–35]) has included studies with cells entrapped in the fibrin gel which are more relevant to tissue engineering. Similarly, studies performed on collagen gels have given insight into the effect of gelation conditions (e.g. temperature, pH) on the collagen microstructure and mechanics [8,36,37]. However, the mechanism by which fibrin and collagen network microstructure and mechanical behavior are changed when formed in the presence of each other, as well as how these ECM networks interact with each other to confer overall mechanical properties to engineered tissue, remains poorly understood. Collagen and fibrin have different gelation mechanisms. Fibrin assembly is initiated by thrombin-catalyzed cleavage of fibrinopeptides from fibrinogen, exposing sites for intermolecular associations between fibrinopeptides to form fibrils [38]. In contrast, collagen fibrils are formed by self-assembly of triple-helical proto-collagen molecules (on the order of 300nm in length) in a staggered formation [39]. Fibrin-collagen composite systems are relevant both physiologically (in the context of wound healing and atherosclerosis [40]) and in bioengineered tissues. Specifically in wound healing, collagen and fibrin play distinct roles: a fibrin clot forms a provisional matrix to stop bleeding, while the process of wound repair involves deposition of newly-synthesized collagen by fibroblasts [41]. Our previous work on collagen-fibrin co-gels [20] focused on the *composition-function* relationship between the two networks, showing non-linearity in mechanical behavior with increasing collagen concentration. In addition, comparison of

mechanical behavior between experimental data and predictions from our computational model showed a transition in collagen-fibrin interactions from series behavior to parallel mechanical behavior as the volume fraction of collagen increased. While the previous study gave some insight into how collagen and fibrin interact in co-gels, those results also raised the question of whether collagen and/or fibrin architecture changes when formed in the presence of each other, and how such changes in morphology alter the mechanics of the co-gels. The purpose of the current study is to investigate the effect of altering network architecture on collagen and fibrin mechanical properties, thereby elucidating *structure-composition-function* relationships between collagen and fibrin in co-gels. We hypothesize that the overall mechanics of collagen-fibrin co-gels is influenced not only by its composition, but also by changes in network architecture of both collagen and fibrin, arising from co-gelation with each other. Specifically, this study investigates changes in microstructure of collagen and fibrin when gelled individually (i.e. in its pure form without a secondary network present) compared to gelation in the presence of each other, and seeks to relate these microstructural changes to alterations in mechanical behavior. To do so, collagen-fibrin co-gels were formed and subsequently subjected to digestion to remove either collagen (with collagenase) or fibrin (with plasmin), while leaving the other network intact. The microstructure and mechanical behavior of these resultant networks were compared with those of their pure counterparts. Scanning Electron Microscopy (SEM) and confocal microcsopy to probe network morphology were coupled with tensile tests to failure to aid in understanding the mechanical behavior of these gels.

MATERIALS AND METHODS

Preparation and Digestion of Collagen, Fibrin, and Collagen-Fibrin Co-gels

The methods for casting collagen, fibrin, and collagen-fibrin co-gels were adapted from [2]. Briefly, 1mL of collagen formulation was comprised of 660μL acid-solubilized rat-tail collagen type I (Life Technologies Corporation - Invitrogen, Grand Island, NY) neutralized with 26 μL of 1M NaOH (Sigma-Aldrich Co. LLC, St Louis, MO), supplemented with 100 μL 10× Minimum Essential Medium (MEM, Sigma-Aldrich), 60 μL fetal bovine serum (Thermo Fisher Scientific Inc. – Hyclone, Logan, UT), 10 μL L-glutamine (Invitrogen), and 1 μL each of penicillin-streptomycin (Invitrogen) and fungizone (Invitrogen). The fibrin formulation consisted of bovine fibrinogen (Sigma-Aldrich) dissolved in 0.02M HEPES buffer (Mediatech Inc, Manassas, VA) in saline (constituting 66% by volume of formulation), polymerized by mixing with a solution containing 0.83%vol thrombin, 0.06%vol Ca^{2+} (Sigma-Aldrich), and 33%vol of 1× DMEM (Mediatech). Collagen-fibrin co-gels (“CG”) were made by mixing 50% by volume of collagen and fibrin formulation. To make pure collagen gels (“C”) with the same collagen concentration as in the co-gels, the above collagen formulation was diluted with an equal amount of 0.5M HEPES buffer (Mediatech). Similarly, pure fibrin gels (“F”) were made by diluting the fibrin formulation with an equal amount of 0.02M HEPES buffer. The gel solutions were cast either into Teflon ring molds (15.5mm OD, 11.5mm ID) for mechanical testing, or Lab-Tek Chambered coverglass slides (Thermo Scientific Inc – Nunc, Rochester, NY) for confocal microscopy. Gels were incubated at 37°C overnight before application of different digestion media.

The digestion protocols are summarized in Table 1. Gels were treated with either 0.02U/mL plasmin (“Pn”) (Sigma-Aldrich), 1U/mL high purity collagenase (“Cs”) (Sigma-Aldrich), or 1× Phosphate-Buffered Saline (“PBS”) (Mediatech). Positive controls to verify the efficacy of the enzymes were performed on pure collagen and pure fibrin gels. All digestion treatments were left overnight at 37°C before further testing or preparation.

Scanning Electron Microscopy (SEM)

Gels were prepared for SEM after digestion treatment using the protocol described in [20]. Briefly, the gels were fixed with 2.5% glutaraldehyde (Electron Microscopy Services, Hatfield, PA), followed by post-fixation staining with 1% osmium tetroxide (Electron Microscopy Services) before sequential dehydration with increasing concentrations of ethanol. The dehydrated samples were freeze-fractured in liquid nitrogen before critical point drying (Tousimis 780A, Tousimis Corp, Rockville, MD) and sputter-coating with platinum. Imaging was performed on a Hitachi S-900 Field Emission Gun SEM (Hitachi High Technologies America Inc, Pleasanton, CA) using a beam voltage of 2kV.

Mechanical Testing

The gel rings were looped over T-bar grips and uniaxially stretched to failure on an Instron 8848 MicroTester (Instron Worldwide Headquarters, Norwood, MA) equipped with a 5N load cell. Before stretch to failure, each ring was stretched to a grip-to-grip length of 14.5mm for 5s. Tensile stretch to failure was performed at a rate of 0.13mm/s. The 1st Piola-Kirchhoff stress (1st PK) was computed by dividing the force data by the cross-sectional area of each gel, estimated based on the volume of gel cast into each ring mold. From plots of 1st PK versus Green strain, the following material properties were calculated: ultimate tensile stress (UTS), Green strain at failure, tangent modulus, and transition strain. At least 6 gels from each digestion condition were tested. How each property is calculated from the stress-strain curve are reported previously [20].

Confocal Microscopy

Indirect immunofluorescence was used to stain the collagen fibrils for confocal microscopy. After the digestion treatments, gels were fixed in 4% paraformaldehyde (Electron Microscopy Services) for 10 minutes, followed by a blocking step with 5% normal donkey serum (Jackson ImmunoResearch, West Grove, PA) for 2 hours. Application of a 1.0mg/mL collagen primary antibody (Novus Biologicals, Littleton, CO) was done overnight at 4°C, at a dilution of 1:100. The next day, gels were incubated with a secondary antibody (Dylight 488, Jackson ImmunoResearch) conjugated with green fluorescent dye at room temperature for one hour. Confocal imaging was performed on a Zeiss Cell Observer SD Spinning Disk Confocal Microscope (Carl Zeiss MicroImaging LLC, Thornwood, NY) with a 100× oil immersion objective. Emission was measured at 488nm, with resolution set at 512 × 512 pixels in-plane and a z-spacing of 0.2μm. The resulting dimensions of the confocal stacks were 133μm × 133μm in-plane with height ranging from 8μm to 10μm in the z-direction.

3-D Network Reconstruction

The confocal image stacks were first deconvoluted using the Huygens software (Scientific Volume Imaging B.V., Netherlands). 3-D reconstructions of the collagen networks in our samples were then generated using the FIbeR Extraction (FIRE) algorithm of [42]. Briefly, image stacks were smoothed using a Gaussian filter to reduce noise, and each pixel was binarized. The threshold value for binarization was determined by the Huygens software by specifying an average background area, i.e. an average pore size. Next, a custom Matlab distance function was used to compute the smallest distance from each fibril pixel to a background pixel. Using the pixels with the largest distance values as nucleation points, fibrils were constructed by tracing from these nucleation points along the maximal ridges of the distance function. From the reconstructed networks, the following network characteristics were analyzed: fiber length, fiber tortuosity, and connectivity around each cross-link. From the total number of fibers (ranging from 2300 to 2900 fibers) and total number of cross-links (1750 to 2650 cross-links), average quantities were also computed. A length-average fiber length, L_L, was also calculated:

$$L_L = \frac{\Sigma L_i^2}{\Sigma L_i} \quad (1)$$

where L_i is the length of fiber *i*. This measure of the average fiber length weights longer fibers more heavily, which captures better the contribution of longer fibers in a non-normal distribution of fiber lengths. It should be noted that collagen *fibrils* cannot be distinguished from collagen *fibers* (from fibril bundling) in these confocal images; hence the term "fiber" refers to both collagen fibrils and fibers in these confocal results.

Statistical Analysis

Statistical comparisons of material properties and network parameters were performed using a 1-way ANOVA F-test, coupled with multiple comparisons using the Bonferroni procedure. Analyses were done using the commercial statistical package in Origin (OriginLab Corporation, Northampton, MA).

RESULTS

Mechanical Testing Results

Figure 1 shows the average failure points of each gel condition after digestion treatments. The data show that failure points are grouped according to their respective network present in the gels: collagen gels (C in PBS, C in Pn, CG in Pn) are clustered in the range of low Green strains around 0.5 to 1, while fibrin gels (F in PBS, F in Cs, CG in Cs) are clustered at higher Green strains between 2.5 to 3.5. That the digested co-gels exhibit similar failure properties to their pure counterparts strongly suggest that the digestion treatments with collagenase and plasmin were effective in eliminating the target network, to the extent that any residual undigested fibrils could not contribute significantly to overall mechanical behavior of the resultant network. The undigested co-gel (CG in PBS) exhibits higher UTS compared to pure collagen and fibrin gels, which is expected since the undigested co-gels have overall protein concentrations that are twice those of the pure gels. More importantly, while the digested co-gels (CG in Pn and CG in Cs) are derivatives of this undigested gel, the failure properties of the undigested gel (CG in PBS) cannot be derived from the sum of the properties of these digested gels.

While the clustering of failure points for each network suggests that both collagen and fibrin retain their general mechanical behavior regardless of gelation condition (i.e. as a pure gel versus in a co-gel) or digestion treatment following gelation, subtle differences are evident when comparing the stress-strain behavior for each network (Figure 2). For the collagen curves (Figure 2A), the digested co-gel (CG in Pn) exhibits a larger toe region and fails at higher strain compared to the pure collagen controls. In addition, a difference was observed between the controls, with the PBS controls (C in PBS) failing at similar strains but significantly higher stresses compared to the negative controls (C in Pn). Comparison of the fibrin curves (Figure 2B) shows similar stress-strain characteristics for all three digestion conditions, with the digested co-gel (CG in Cs) failing at higher strains but similar stresses compared to the controls. Figure 3 shows further comparison of the mechanical behavior of the various gels in terms of their Green strains at failure (Figure 3A), UTS (Figure 3B), tangent modulus (Figure 3C) and transition strain (Figure 3D). The longer toe region seen in the collagen network after co-gel digestion (CG in Pn) from Figure 2A is shown by the larger transition strain compared to controls (Figure 3D). In addition, the higher stresses seen in the collagen PBS controls are manifested in statistically significant differences in UTS and tangent modulus when compared to the negative controls (C in Pn). Overall, similar statistical trends were observed for both collagen and fibrin: the digested co-gels

exhibited higher failure strains, similar UTS, and lower tangent modulus when compared to their pure component counterparts (both PBS and negative controls). These comparisons are statistically significant at the 95% confidence level, with the exception of Green strain at failure for fibrin between the digested co-gel (CG in Ce) and PBS control (F in PBS) which is significant at the 90% level (p-value = 0.067).

Microstructural Results

Figure 4 shows SEM images of the gels after digestion. Images of the negative controls of pure collagen (C in Pn) and pure fibrin (F in Cs) appear similar to their respective PBS controls (C in PBS and F in PBS), which suggests that the network microstructures were not affected by the digestion media. Comparison of the pure collagen and pure fibrin networks show that both protein matrices qualitatively exhibit similar diameters; closer inspection of these images (see Supplementary Material for larger images) revealed characteristic banding on the collagen fibrils, absent in the fibrin fibrils. The co-gel control (CG in PBS), however, exhibits distinct differences in fibril diameters: finer, wisp-like structures can be seen in addition to the fibrils of similar thickness to those observed in the pure collagen and fibrin images (representative fibril diameters shown by arrows → ←). These wispy, web-like structures are still prevalent after the collagen had been digested (CG in Cs), strongly indicating that these structures are fibrin fibrils. Qualitatively, the distribution of fibril diameters of collagen appears similar in the digested co-gel (i.e. CG in Pn) compared to the pure collagen gels, although less bundling is observed (denoted by * in images) between the fibrils such that *fiber* diameters appeared smaller in these digested co-gels. Finer fibrils can also be seen in the CG in Pn co-gel, albeit much less prevalent than in the fibrin-remaining co-gel (CG in Cs). While we are unable to discern whether these finer fibrils are collagen or fibrin, we believe that they are primarily residual fibrin fibrils that were not digested. Collectively, comparison of SEM images suggests that both collagen and fibrin network morphologies are altered when formed in the presence of each other: fibrin fibril diameter decreases, and collagen fibrils exhibit less bundling.

To analyze further network differences in the collagen networks, 3-D reconstruction of these networks using confocal image stacks of the collagen gels were performed. Figure 5 shows a representative 3-D image of a reconstructed collagen network (C in Pn) (top), as well as the comparison between the collapsed confocal image stack (bottom) before deconvolution (left), after deconvolution (middle), and the reconstructed network (right). It should be reiterated that collagen fibrils cannot be differentiated from collagen fibers (bundled fibrils) in these confocal images, such that the term “fiber” refers collectively to both fibrils and bundled fibers. Comparison of the collapsed images before and after deconvolution indicates that while the deconvolution process makes fibers more distinct by removing the spread in fluorescence, fibers also appear more fragmented as a result. These fragmented fibers are re-connected during the network reconstruction process via the FIRE algorithm, where fiber segments of similar orientation are extended as the same fiber. Comparison between the reconstructed network and deconvoluted network shows good qualitative agreement, in general, in network morphology. Results analyzing network morphologies of the different conditions are shown in Figure 6, comparing total fiber length per volume (A), average connectivity around a cross-link (B), average *segment* length and tortuosity (C and D), and average *fiber* length and tortuosity (E and F). A *segment* is defined as the spacing between cross-links, while a *fiber* can be comprised of multiple adjacent segments of similar orientation (see Figure 7 for an illustration). The minimum value allowable between 2 segments to be considered part of the same fiber (i.e. angle α in Figure 7) was set at 120°. This value was determined via a sensitivity analysis examining the effect of varying α on the total number of cross-links with connectivity of only 2 (data not shown). Since cross-links of connectivity of 2, formed by contact between two fibril ends, were expected to be

very uncommon, a large jump in the number of such cross-links (which occurred between 120° and 130°) suggested at α values greater than 120°, several fibers had been artificially broken up into two fibers. In general, no significant differences in network characteristics were observed between samples formed under the same gelation condition, but placed in different digestion medium (i.e. CG in Pn vs CG in PBS, and C in Pn vs C in PBS). Assuming the same collagen density for all samples, the total fiber length per volume (Figure 6A) provides a crude measure of fiber diameter, with the higher values in the co-gels (CG in P, CG in PBS) indicating *smaller* average fiber diameters compared to the pure gels (C in Pn, C in PBS). In addition, the collagen networks formed in the co-gels also exhibited higher average connectivities (Figure 6B) compared to the pure gels (* indicates statistical significance at the 95% level). While no significant differences were observed in average segment length (Figure 6C) and average segment tortuosity (Figure 6D) between the co-gels and pure gels, the collagen network in co-gels exhibited longer average fiber lengths (Figure 6E) but similar fiber tortuosities (Figure 6F) than the networks in the pure gels.

To investigate these differences in connectivities and fiber lengths further, their distributions were analyzed in Figures 8 and 9, respectively. The distribution of connectivities comprises integer values which spanned a narrow range from 2 to 12. Figure 8A shows similar overall distributions of connectivities across all samples, with more than 80% of crosslinks having connectivities of 3 or 4. The collagen networks from co-gels (CG in Pn, CG in PBS) exhibiting a slightly higher proportion of crosslinks with connectivities 5 or greater. The box-plot in Figure 8B shows that key differences in connectivity distributions occur only above the 90^{th} percentile (top of whisker): the collagen networks in co-gels exhibited higher connectivities at the 99^{th} (●) percentile and had larger maximum connectivity values (▲). Collectively, these results explain the higher average connectivities in the co-gels (CG in P, CG in PBS): these networks have *more crosslinks that have higher connectivities*. Figure 9 shows similar analysis for the fiber length distributions in the collagen networks, with Figure 9A showing an example of the non-normal distribution of fiber lengths. The right-skewed distribution in all the samples is evidenced by the lower median value (middle line in box) compared to the mean (■) in the box-plot in Figure 9B. While all four samples showed similar fiber lengths at the 25^{th}, 50^{th} and 75^{th} percentiles (i.e. in the box region), longer fiber lengths at the 90^{th} (top of whisker) and 99^{th} percentile (•) were observed for the networks in the co-gels compared to those in the pure gels. These results suggest that the longer average fiber lengths in the networks from co-gels (Figure 6F) are not due to a general increase in length of all fibers, but due to the *presence of very long fibers* in the co-gel networks. Comparison of the length-average fiber length (Figure 9C) confirms this result, as the difference in fiber lengths between the networks in co-gels vs networks in pure gels is further accentuated when longer fibers are weighted more heavily.

DISCUSSION

This study investigated the effect of collagen-fibrin co-gelation on the network morphologies of each network, and how such changes in network architecture influenced overall mechanical behavior. Upon digestion of the collagen-fibrin co-gels with either plasmin or collagenase, a network of the undigested ECM remained in the gel. This observation suggests extensive end-to-end crosslinking between collagen and fibrin fibrils or monomers did not occur; instead, each biopolymer formed its own network that interpenetrated with the other in a “parallel” fashion. In addition, results showed effects on microstructure and mechanics of both collagen and fibrin when these ECM are co-gelated in the presence of each other (as summarized in Table 2):

Fibrin: Microstructural results from SEM images showed a finer network containing web-like/wispy structures, which apparently are fibrin fibrils, when the fibrin network is co-

gelated with collagen. This observation is consistent with previous studies which showed that fibrin morphology was sensitive to gelation conditions such as thrombin and Ca^{2+} concentrations [26,31,32]. Furthermore, we had also shown previously the existence of such finer fibrin fibrils in collagen-fibrin co-gels, although these were only observed at higher collagen concentrations [20]. Mechanically, fibrin formed in the co-gels exhibited similar failure strength, lower modulus, but greater extensibility before failure. Correlation of SEM results with these mechanical data for fibrin suggested that, in general, a decrease in fibril diameter resulted in a more compliant gel of similar tensile strength, but greater extensibility before failure. This result is contrary to previous findings of Rowe et al. [32], who found that a decrease in fibril diameter (formed by decreasing thrombin concentration) effected an increase in UTS and modulus. It should be noted that, however, the microstructural changes caused by altering thrombin concentrations in that study were significantly more drastic; SEM images from [32] showed that as fibril diameter decreased with decreasing thrombin concentration, the overall network became much more highly interconnected with smaller pores, leading to an increase in mechanical strength and stiffness. In contrast, our SEM images of fibrin networks under different conditions at lower magnifications of 10,000× (see Supplementary Material) showed no visible differences in network architecture. Previous studies on fibrin networks suggest that thicker fibrin fibrils are formed from lateral associations of thinner fibrils, with possible inter-fibril γ chain cross-linking [38]. Conceivably, the smaller failure strain observed in the pure fibrin gels (F in PBS, F in Cs) is due to decreased extensibility of these thicker fibrils as the inter-fibril cross-links hinder stretch of individual fibrils within these fibers. The lower stretch borne by these thicker fibrils necessitates that the thinner fibrils bear a larger proportion of the overall macroscopic stretch, causing catastrophic failure to occur at lower strains. In addition, these inter-fibril cross-links could also stiffen fibrin bundles compared to individual fibrils, resulting in an overall network with slightly higher modulus.

Collagen: Similar trends in microstructure and mechanics were observed for our collagen networks when formed in the presence of fibrin (CG in Pn) compared to formation in its absence (C in Pn, C in PBS): SEM images showing a decrease in average collagen fibril and fiber diameter were accompanied by mechanical data showing similar failure strength, higher strain at failure, and lower tangent modulus. A similar explanation could be made to correlate microstructure with mechanics, that inter-fibrillar bonding between collagen fibrils in bundled fibers [43] (i.e. bonding between laterally associated fibrils within fibers) decreased overall extensibility while increasing stiffness. Further analysis into the collagen network from the reconstructed networks confirmed the result of smaller average collagen fibril/fiber diameters (cf. Figure 6A). In addition, while the collagen networks in co-gels showed higher average connectivities, this result was due to the *greater presence of cross-links with very high connectivities* rather than a general increase in connectivity throughout all cross-links. In all cases, connectivities around each cross-link of 3 or 4 were predominant. A connectivity of 3 suggests branching of collagen fibers from a bundled fiber, a phenomenon also observed from cryo-SEM of collagen networks [43]. A cross-link with connectivity 4 can be formed by two fibrils crossing at close proximity to each other and forming an inter-fibrillar chemical bond, or fibrils intertwining to form a mechanical bond. Connectivities above 4 are likely a result of clumping of fibrils, with fibrils radiating out from a central cluster as the FIRE code is unable to resolve fibrils within the cluster. Results from this study suggest that, in general, collagen networks formed in the presence of fibrin retain similar cross-link characteristics compared to collagen networks formed purely by themselves, with similar spacings and tortuosities between cross-links (i.e. segment lengths, cf. Figure 6C and 6D), and predominantly connectivities of 3 or 4. The very high connectivities observed for the collagen networks in co-gels (Figure 8B) suggest more clustering of collagen fibrils when formed with fibrin.

Several groups have previously studied the correlation between collagen network microstructure and overall mechanical behavior of collagen gels. Notable works include the study by Christiansen and co-workers [8], who investigated the effect of pH and temperature on collagen network formation. In that study, they reported a decrease in collagen fibril diameter with increasing pH from 5.0 to 9.0; comparison with mechanical properties showed that an increase in collagen fibril diameter correlated well with an increase in low strain modulus, but had no effect on UTS or high strain modulus. A similar study by Roeder et al. [37] confirmed the decrease in collagen fibril diameter with increasing pH, as well as an increase in fibril length. However, the group reported an accompanying increase in UTS and linear modulus, results that were contrary to Christiansen et al.. Roeder and co-workers concluded that collagen fibril length had a greater effect on mechanical properties than fibril diameter. In the current study, co-gelation of collagen with fibrin yielded longer but less bundled collagen fibers (i.e. smaller fiber diameter); however, like Christiansen et al., no significant increase in UTS was observed. In contrast to Roeder et al., results from this study suggest a greater effect of collagen fibril diameter than fibril length – thicker fibers reduce macroscopic extensibility and increase overall gel stiffness, presumably due to inter-fibrillar bonding in fiber bundles. It should be noted that all three studies employed similar strain rates for mechanical testing, so that these differences are not due to the viscoelastic nature of these gels. Such discrepancies among reported results highlight the complexity of biological networks: changes in microstructure alone cannot fully account for changes in macroscopic mechanical properties. Different gelation conditions such as variations in pH and presence of contaminants could have affected fibrils on a molecular level, e.g. the degree of cross-linking and bonding between fibrils – factors that cannot be visualized using SEM or confocal microscopy.

Mechanical data for collagen networks revealed additional differences absent in fibrin networks. Firstly, the collagen PBS control (C in PBS) exhibited a higher UTS compared to the gels placed in plasmin (C in Pn, CG in Pn). While positive controls were carried out to verify efficacy of the enzymes used – pure collagen and fibrin gels were fully dissolved when placed in collagenase and plasmin respectively, the plasmin could have caused slight degradation of the collagen network and reduced the strength of the gel even though the collagen network remained largely intact. Secondly, the collagen gels formed by co-gelation with fibrin showed significantly larger transition strains, i.e. these gels have a longer toe region. Previous studies suggest that the toe region corresponds to straightening of undulating fibrils at the fibrillar level [9] and the molecular level [44], as well as fibril reorientation in the direction of stretch [45,46]. Results from this study showed similar fiber and segment tortuosities between collagen networks in co-gels and in pure gels, which indicated that this longer toe region in co-gels could not be explained by more curved fibrils on the fibrillar level. Whether the longer toe region was caused by differences at the molecular level, or due to changes in network characteristics more conducive for fibril rearrangement, remains unclear.

The combination of SEM and confocal imaging techniques allowed observation of collagen networks both at the fibril level and at the network level. However, visual comparisons of images from these techniques showed straighter fibers and larger void spaces in the confocal images compared to SEM. We believe that these discrepancies are due to structural artifacts introduced during sample preparation for SEM; the drying process is known to cause slight network collapse resulting in smaller void spaces [47]. Nevertheless, SEM images provide useful qualitative information on our networks at the fibrillar level such as collagen fiber bundling and wispy fibrin fibrils.

Previous studies have shown that gelation conditions of pH and ionic strength influenced fibril formation of both fibrin [25] and collagen [36], resulting in varied microstructures.

The formulations used to prepare the gels for these studies varied from each other such that slight differences in pH and ionic concentration were observed between the formulations (Table 3). While the pH of all three formulations were maintained close to neutrality, there was significant difference in the ionic strength of pure collagen (C; 0.12M) compared to that in the co-gel (CG; 0.16M). Wood and Keech [36] reported that an increase in ionic strength from 0.13M to 0.23M effected an increase in collagen fibril diameter; more extensive fibril bundling was also observed. In contrast, an opposite trend for changes in collagen microstructure was observed in our gels: an increase in ionic strength from 0.12M (in pure collagen) to 0.16M (in the collagen-fibrin co-gel) resulted in less fibril bundling and a decrease in average fibril diameter. These different findings highlight the intricate effects of gelation conditions on collagen microstructure and warrants further investigation.

Results from this study indicated that while averaged characteristics are useful in quantifying gross differences in overall network architecture, they do not give the full picture of how the network morphology is changed. Thus, these findings are also relevant towards improving modeling approaches to understand the mechanics of certain native and bioengineered tissues where a collagen-fibrin co-gel is a relevant experimental model. Different groups have used a variety of approaches to model fiber networks, ranging from periodic [48] or homogeneously distributed fiber models [49], to known models for disordered networks, e.g. the Poisson-Voronoi model [50]. To model the mechanical contribution of the ECM in tissues, our group employs a multi-scale framework using a Representative Volume Element (RVE) containing a fiber network around each Gauss point [51,52]. This current method network generation in the RVEs creates a randomly orientated network of elastic fibers connected to one another via rigid pin joints [51]. While our current network models are able to capture the inhomogeneous and anisotropic nature of ECM fiber networks, they suffer the same limitation as the afore-mentioned approaches: these networks do not accurately reflect the microstructure of the ECM networks in the tissues. Here we utilized a method of characterizing ECM networks developed by Stein et al. via 3-D reconstruction of confocal z-stacks and fiber network analysis to obtain actual ECM network characteristics (connectivities, fiber length distributions, fiber tortuosities etc), which can be used to improve our network generation approaches to create fiber networks that mimic more closely the actual microstructure of the ECM in tissues.

Supplementary Material

Refer to Web version on PubMed Central for supplementary material.

Acknowledgments

The authors gratefully acknowledge financial support from the National Institutes of Health (R01-EB005813) and the American Heart Association (11PRE5410003). We thank Guillermo Marquez from the University Imaging Center for his help with the Spinning Disk Confocal Microscope, and Dr. Andy Stein for providing the FIRE code. Parts of this work were carried out in the Characterization Facility, University of Minnesota, which receives partial support from NSF through the MRSEC program.

REFERENCES

1. Prockop JD. Collagens: Molecular biology, diseases, and potentials for therapy. Annu Rev Biochem. 1995; 64:403–434. [PubMed: 7574488]
2. Cummings CL, Gawlitta D, Nerem RM, Stegemann JP. Properties of engineered vascular constructs made from collagen, fibrin, and collagen–fibrin mixtures. Biomaterials. 2004; 25:3699–3706. [PubMed: 15020145]

3. Buttafoco L, Kolkman NG, Engbers-Buijtenhuijs P, Poot AA, Dijkstra PJ, Vermes I, Feijen J. Electrospinning of collagen and elastin for tissue engineering applications. Biomaterials. 2006; 27:724–734. [PubMed: 16111744]
4. Grassl ED, Oegema TR, Tranquillo RT. Fibrin as an alternative biopolymer to type-I collagen for the fabrication of a media equivalent. J Biomed Mater Res. 2002; 60:607–612. [PubMed: 11948519]
5. Ross J, Tranquillo R. ECM gene expression correlates with in vitro tissue growth and development in fibrin gel remodeled by neonatal smooth muscle cells. Matrix Biol. 2003; 22:477–490. [PubMed: 14667840]
6. Robinson PS, Johnson SL, Evans MC, Barocas VH, Tranquillo RT. Functional tissue-engineered valves from cell-remodeled fibrin with commissural alignment of cell-produced collagen. Tissue Eng Part A. 2008; 14:83–95. [PubMed: 18333807]
7. Syedain ZH, Weinberg JS, Tranquillo RT. Cyclic distension of fibrin-based tissue constructs: evidence of adaptation during growth of engineered connective tissue. Proc Natl Acad Sci. 2008; 105:6537–6542. [PubMed: 18436647]
8. Christiansen DL, Huang EK, Silver FH. Assembly of type I collagen: fusion of fibril subunits and the influence of fibril diameter on mechanical properties. Matrix Biol. 2000; 19:409–420. [PubMed: 10980417]
9. Diamant J, Keller A, Baer E, Litt M, Arridge RGC. Collagen; ultrastructure and its relation to mechanical properties as a function of ageing. Proc R Soc Lond [Biol]. 1972; 180:293–315.
10. Eppell SJ, Smith BN, Kahn H, Ballarini R. Nano measurements with micro-devices: mechanical properties of hydrated collagen fibrils. J R Soc Interface. 2006; 3:117–121. [PubMed: 16849223]
11. Liu W, Jawerth LM, Sparks EA, Falvo MR, Hantgan RR, Superfine R, Lord ST, Guthold M. Fibrin Fibers have extraordinary extensibility and elasticity. Science. 2006; 313:634. [PubMed: 16888133]
12. Mosesson MW. Fibrinogen and fibrin structure and functions. J Thromb Haemost. 2005; 3:1894–1904. [PubMed: 16102057]
13. Roska FJ, Ferry JD. Studies of fibrin film. I. Stress relaxation and birefringence. Biopolymers. 1982; 21:1811–1832. [PubMed: 7126757]
14. Roska FJ, Ferry JD, Lin JS, Anderegg JW. Studies of fibrin film. II. Small-angle x-ray scattering. Biopolymers. 1982; 21:1833–1845. [PubMed: 7126758]
15. Pezzin G, Scandola M, Gotte L. The low temperature mechanical relaxation of elastin. I. The dry protein. Biopolymers. 1976; 15:283–292. [PubMed: 1247656]
16. Scandola M, Pezzin G. The low temperature mechanical relaxation of elastin. II. The solvated protein. Biopolymers. 1978; 17:213–223. [PubMed: 623881]
17. Yonese M, Baba K, Kishimoto H. Viscoelastic properties of poly(vinyl alcohol)/alginate snake-cage hydrogels and interpenetrating hydrogels. Polym J. 1992; 24:395–404.
18. Mathew AP, Packirisamy S, Thomas S. Morphology, mechanical properties, and failure topography of semi-interpenetrating polymer networks based on natural rubber and polystyrene. J Appl Polym Sci. 2000; 78:2327–2344.
19. Santin M, Huang SJ, Iannace S, Ambrosio L, Nicolais L, Peluso G. Synthesis and characterization of a new interpenetrated poly(2-hydroxyethylmethacrylate)—gelatin composite polymer. Biomaterials. 1996; 17:1459–1467. [PubMed: 8853115]
20. Lai VK, Lake SP, Frey CR, Tranquillo RT, Barocas VH. Mechanical Behavior of Collagen-Fibrin Co-Gels Reflects Transition From Series to Parallel Interactions With Increasing Collagen Content. J Biomech Eng. 2012; 134 011004.
21. Rowe SL, Stegemann JP. Interpenetrating collagen-fibrin composite matrices with varying protein contents and ratios. Biomacromolecules. 2006; 7:2942–2948. [PubMed: 17096517]
22. Mosher DF, Schad PE. Cross-linking of fibronectin to collagen by blood coagulation Factor XIIIa. J Clin Invest. 1979; 64:781–787. [PubMed: 38260]
23. Stemberger A, Jilek F, Hormann H, Blumel G. Fibrinogen-collagen interactions. Thromb Haemostasis. 1977; 38:305.
24. Duckert F, Nyman D. Factor XIII, fibrin and collagen. Suppl Thromb Haemost. 1978; 63:391–396. [PubMed: 262335]

25. Ferry JD, Morrison PR. Preparation and Properties of Serum and Plasma Proteins. VIII. The Conversion of Human Fibrinogen to Fibrin under Various Conditions. J Am Chem Soc. 1947; 69:388–400. [PubMed: 20292443]
26. Blombäck B, Carlsson K, Fatah K, Hessel B, Procyk R. Fibrin in human plasma: Gel architectures governed by rate and nature of fibrinogen activation. Thromb Res. 1994; 75:521–538. [PubMed: 7992253]
27. Blombäck B, Carlsson K, Hessel B, Liljeborg A, Procyk R, Åslund N. Native fibrin gel networks observed by 3D microscopy, permeation and turbidity. Biochim Biophys Acta, Protein Struct Mol Enzymol. 1989; 997:96–110.
28. Akpalo E, Larreta-Garde V. Increase of fibrin gel elasticity by enzymes: A kinetic approach. Acta Biomaterialia. 2010; 6:396–402. [PubMed: 19664730]
29. Shen LL, McDonagh RP, McDonagh J, Hermans J Jr. Fibrin gel structure: influence of calcium and covalent cross-linking on the elasticity. Biochem Biophys Res Commun. 1974; 56:793–798. [PubMed: 4207907]
30. Kaibara M, Fukada E. Effect of temperature on dynamic viscoelasticity during the clotting reaction of fibrin. Biochim Biophys Acta, Gen Subj. 1977; 499:352–361.
31. Dubey N, Letourneau PC, Tranquillo RT. Neuronal contact guidance in magnetically aligned fibrin gels: effect of variation in gel mechano-structural properties. Biomaterials. 2001; 22:1065–1075. [PubMed: 11352087]
32. Rowe SL, Lee SY, Stegemann JP. Influence of thrombin concentration on the mechanical and morphological properties of cell-seeded fibrin hydrogels. Acta Biomater. 2007; 3:59–67. [PubMed: 17085089]
33. Naito M, Nomura H, Iguchi A, Thompson WD, Smith EB. Effect of crosslinking by factor XIIIa on the migration of vascular smooth muscle cells into fibrin gels. Thromb Res. 1998; 90:111–116. [PubMed: 9684729]
34. Mol A, van Lieshout MI, Dam-de Veen CG, Neuenschwander S, Hoerstrup SP, Baaijens FPT, Bouten CVC. Fibrin as a cell carrier in cardiovascular tissue engineering applications. Biomaterials. 2005; 26:3113–3121. [PubMed: 15603806]
35. Ho W, Tawil B, Dunn JCY, Wu BM. The behavior of human mesenchymal stem cells in 3D fibrin clots: dependence on fibrinogen concentration and clot structure. Tissue Eng. 2006; 12:1587–1595. [PubMed: 16846354]
36. Wood GC, Keech MK. The formation of fibrils from collagen solutions 1. The effect of experimental conditions: kinetic and electron-microscope studies. Biochem J. 1960; 75:588–598. [PubMed: 13845809]
37. Roeder BA, Kokini K, Sturgis JE, Robinson JP, Voytik-Harbin SL. Tensile Mechanical properties of three-dimensional type I collagen extracellular matrices with varied microstructure. J Biomech Eng. 2002; 124:214–222. [PubMed: 12002131]
38. Mosesson MW, Siebenlist KR, Meh DA. The structure and biological features of fibrinogen and fibrin. Ann NY Acad Sci. 2001; 936:11–30. [PubMed: 11460466]
39. Kadler KE, Holmes DF, Trotter JA, Chapman JA. Collagen fibril formation. Biochem J. 1996; 316:1–11. [PubMed: 8645190]
40. Eb S. Fibrinogen, fibrin and fibrin degradation products in relation to atherosclerosis. Clin Haematol. 1986; 15:355. [PubMed: 3524931]
41. Martin P. Wound Healing--Aiming for perfect skin regeneration. Science. 1997; 276:75–81. [PubMed: 9082989]
42. Stein AM, Vader DA, Jawerth LM, Weitz DA, Sander LM. An algorithm for extracting the network geometry of three-dimensional collagen gels. J Microsc. 2008; 232:463–475. [PubMed: 19094023]
43. Lewis JL, Johnson SL, Oegema TR. Interfibrillar collagen bonding exists in matrix produced by chondrocytes in culture: evidence by electron microscopy. Tissue Eng. 2002; 8:989–995. [PubMed: 12542944]
44. Fratzl P, Misof K, Zizak I, Rapp G, Amenitsch H, Bernstorff S. Fibrillar structure and mechanical properties of collagen. J Struct Biol. 1998; 122:119–122. [PubMed: 9724612]

45. Chandran PL, Barocas VH. Microstructural mechanics of collagen gels in confined compression: poroelasticity, viscoelasticity, and collapse. J Biomech Eng. 2004; 126:152–166. [PubMed: 15179845]

46. Tower TT, Neidert MR, Tranquillo RT. Fiber alignment imaging during mechanical testing of soft tissues. Ann Biomed Eng. 2002; 30:1221–1233. [PubMed: 12540198]

47. Stuart K, Panitch A. Influence of chondroitin sulfate on collagen gel structure and mechanical properties at physiologically relevant levels. Biopolymers. 2008; 89:841–851. [PubMed: 18488988]

48. Purohit PK, Litvinov RI, Brown AEX, Discher DE, Weisel JW. Protein unfolding accounts for the unusual mechanical behavior of fibrin networks. Acta Biomater. 2011; 7:2374–2383. [PubMed: 21342665]

49. Soulhat J, Buschmann MD, Shirazi-Adl A. A fibril-network-reinforced biphasic model of cartilage in unconfined compression. J Biomech Eng. 1999; 121:340–347. [PubMed: 10396701]

50. Nachtrab S, Kapfer SC, Arns CH, Madadi M, Mecke K, Schröder-Turk GE. Morphology and Linear-elastic moduli of random network solids. Adv Mater. 2011; 23:2633–2637. [PubMed: 21681832]

51. Stylianopoulos T, Barocas VH. Volume-averaging theory for the study of the mechanics of collagen networks. Comput Meth Appl Mech Eng. 2007; 196:2981–2990.

52. Sander EA, Stylianopoulos T, Tranquillo RT, Barocas VH. Image-based multiscale modeling predicts tissue-level and network-level fiber reorganization in stretched cell-compacted collagen gels. Proc Natl Acad Sci. 2009; 106:17675–17680. [PubMed: 19805118]

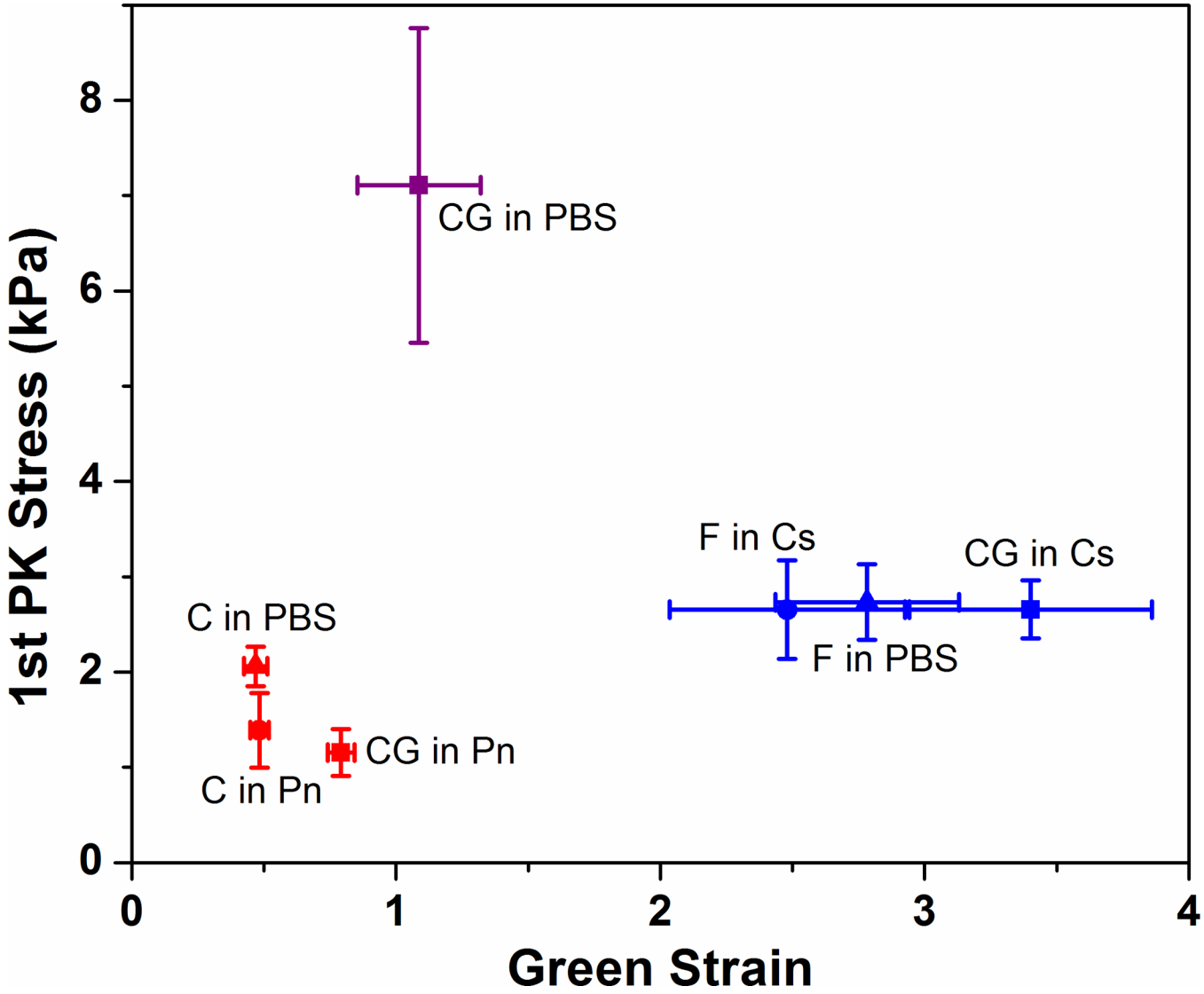

Figure 1.
Failure points of stress-strain curves for all samples with different digestion conditions. Clustering of failure points for each network (collagen networks at lower strains, fibrin networks at higher strains) indicate that digestion with collagenase or plasmin was effective in eliminating the target network. The un-digested co-gel (CG in PBS) exhibited significantly higher failure stress because it contained twice the protein concentration compared to all other gels. Error bars represent 95% confidence intervals, $n \geq 6$ for all samples.

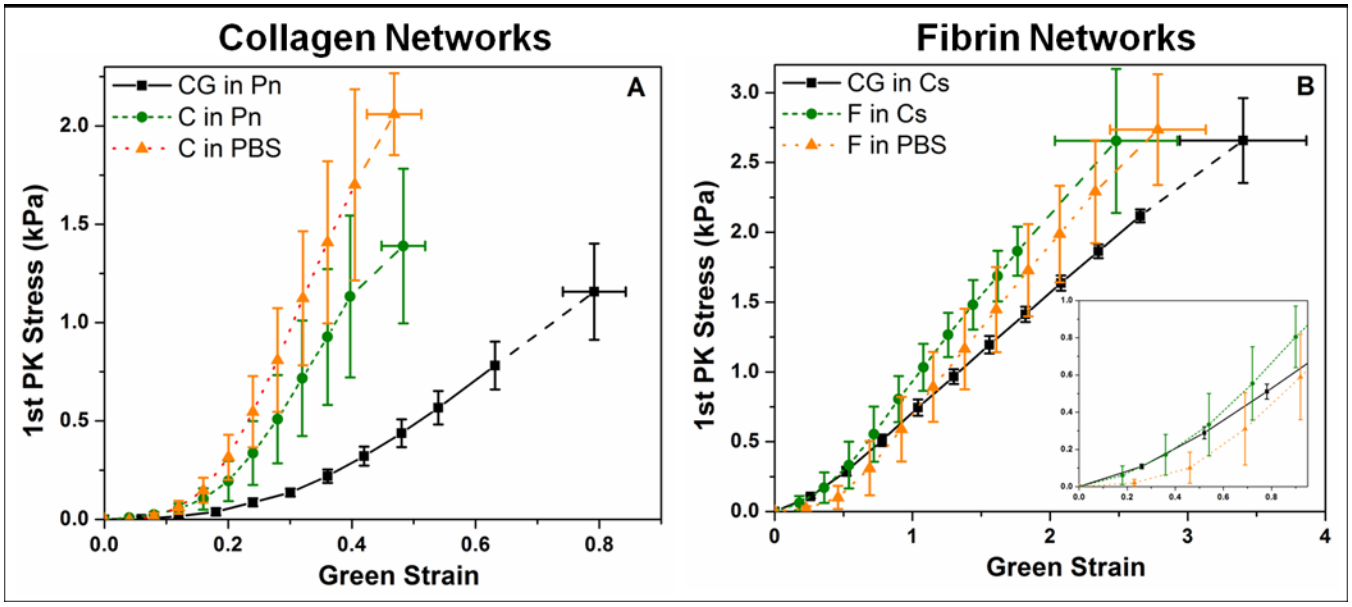

Figure 2.

Stress-strain curves of (A) collagen, and (B) fibrin networks. Fibrin networks fail at much higher strains than collagen networks; inset in (B) shows the magnification of the fibrin curves up to the failure strains of the collagen networks. Both networks formed from digestion of co-gels (CG in Pn, CG in Cs) exhibited higher failure strains compared to their pure counterparts. Collagen PBS control (C in PBS) shows higher failure stress than gels in plasmin (C in Pn, CG in Pn). Error bars represent 95% confidence intervals, $n \geq 6$ for all samples.

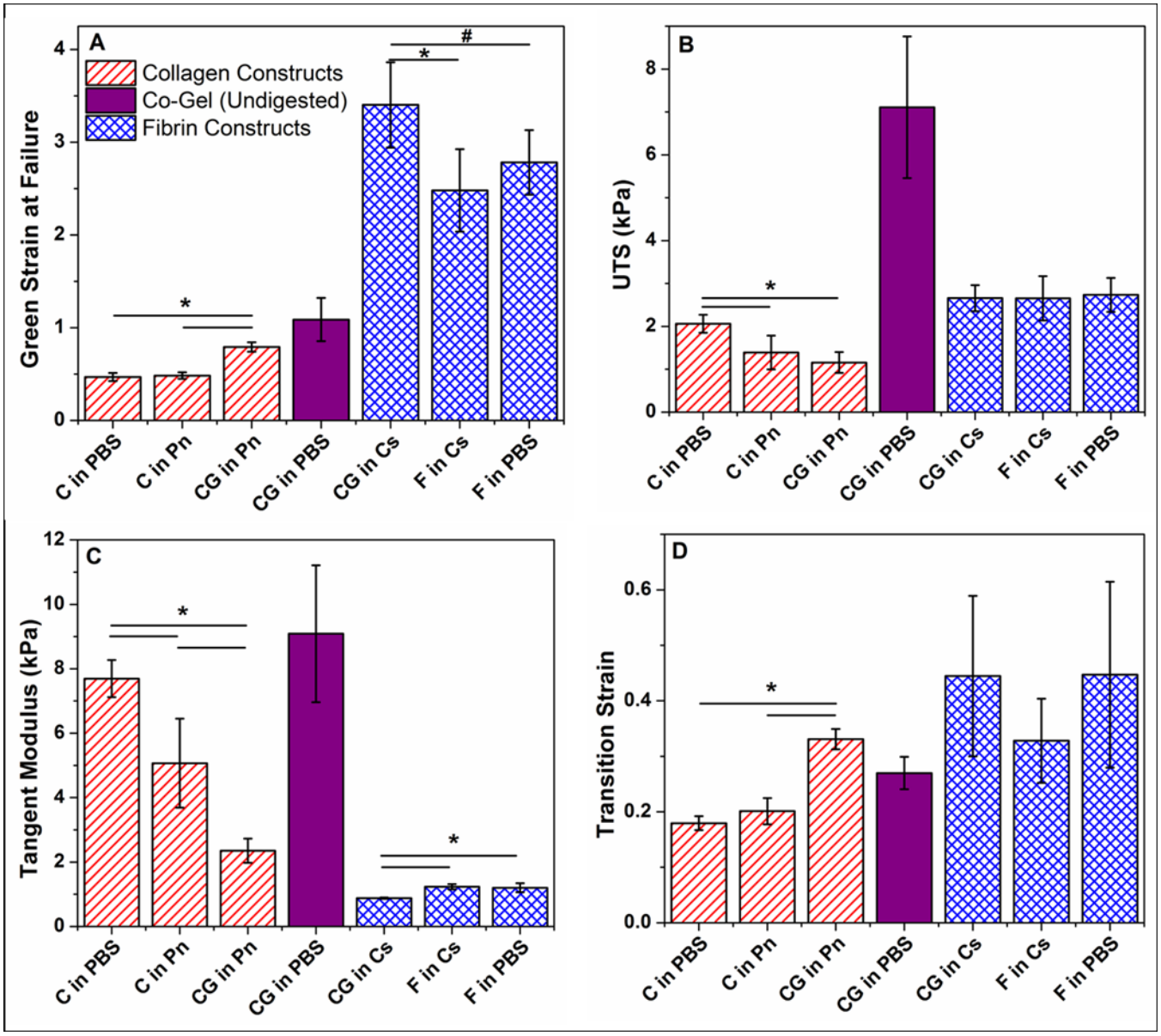

Figure 3.

Comparison of material properties of (A) Green strain at failure, (B) ultimate tensile stress (UTS), (C) tangent modulus, and (D) transition strain between collagen and fibrin networks under different digestion conditions. In general, collagen and fibrin networks obtained from co-gel digestion exhibited similar UTS, but higher failure strains and lower tangent modulus when compared to their pure counterparts. Material properties of the undigested co-gel (CG in PBS) cannot be derived from the sum of properties of the digested co-gels (CG in Pn, CG in Cs), showing the the rule of mixtures does of apply to these collagen-fibrin systems. Error bars represent 95% confidence intervals, $n \geq 6$ for all samples. * and # represent statistical significance at the 95% and 90% levels respectively.

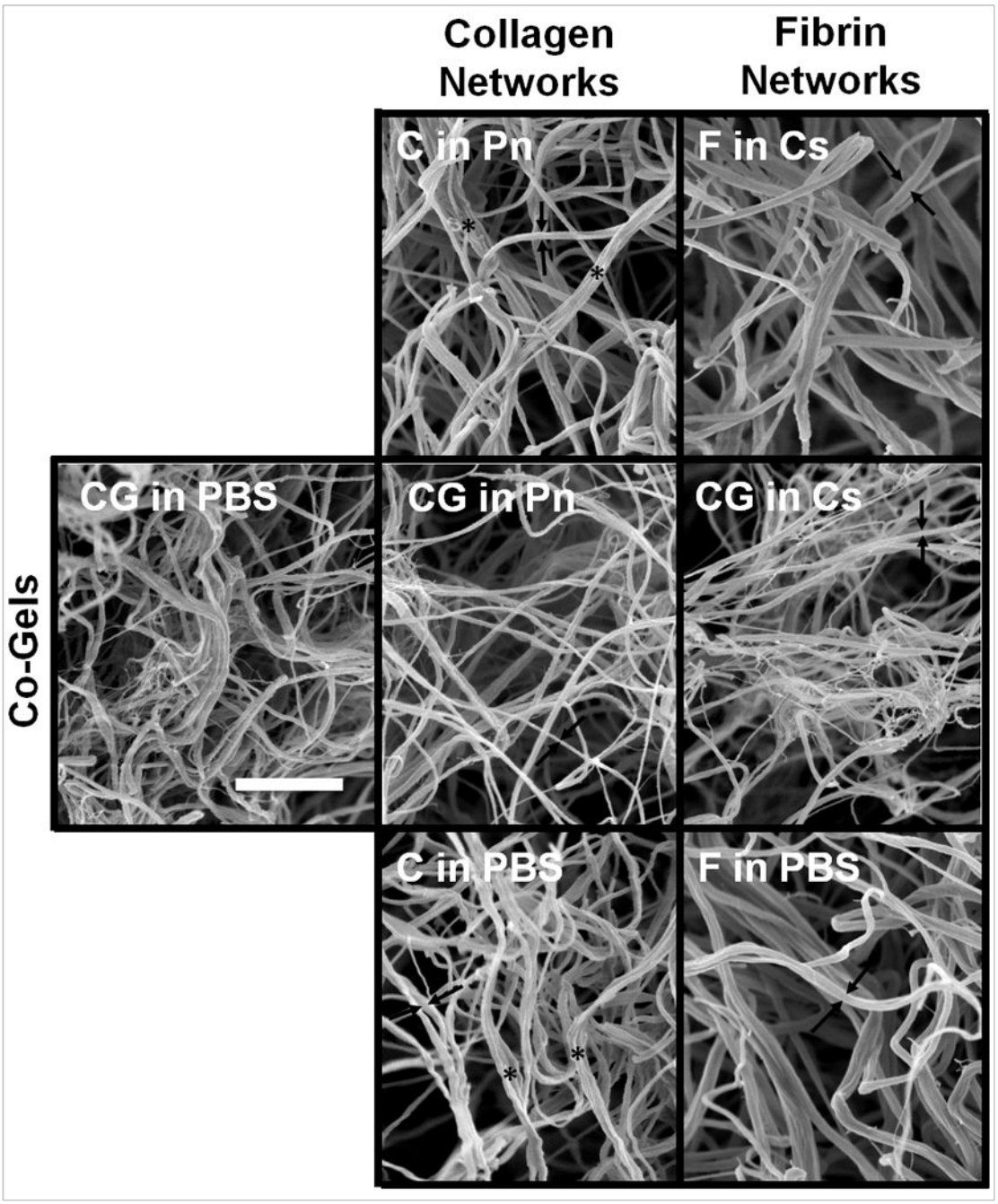

Figure 4.

SEM images taken at 30,000× of collagen (2nd column) and fibrin (3rd column) networks under different digestion conditions; samples obtained from co-gels showed in middle row. The collagen network from co-gel digestion (CG in P) showed less fibril bundling (indicated with * on images) than the pure collagen gels, and have slightly smaller average fibril diameters The fibrin network from co-gel digestion (CG in Cs) contained wispy, web-like structures absent in the pure fibrin gels. Arrows (→ ←) on images denote representative fibril diameter for each gel. Scale bar = 1μm and is representative for all images.

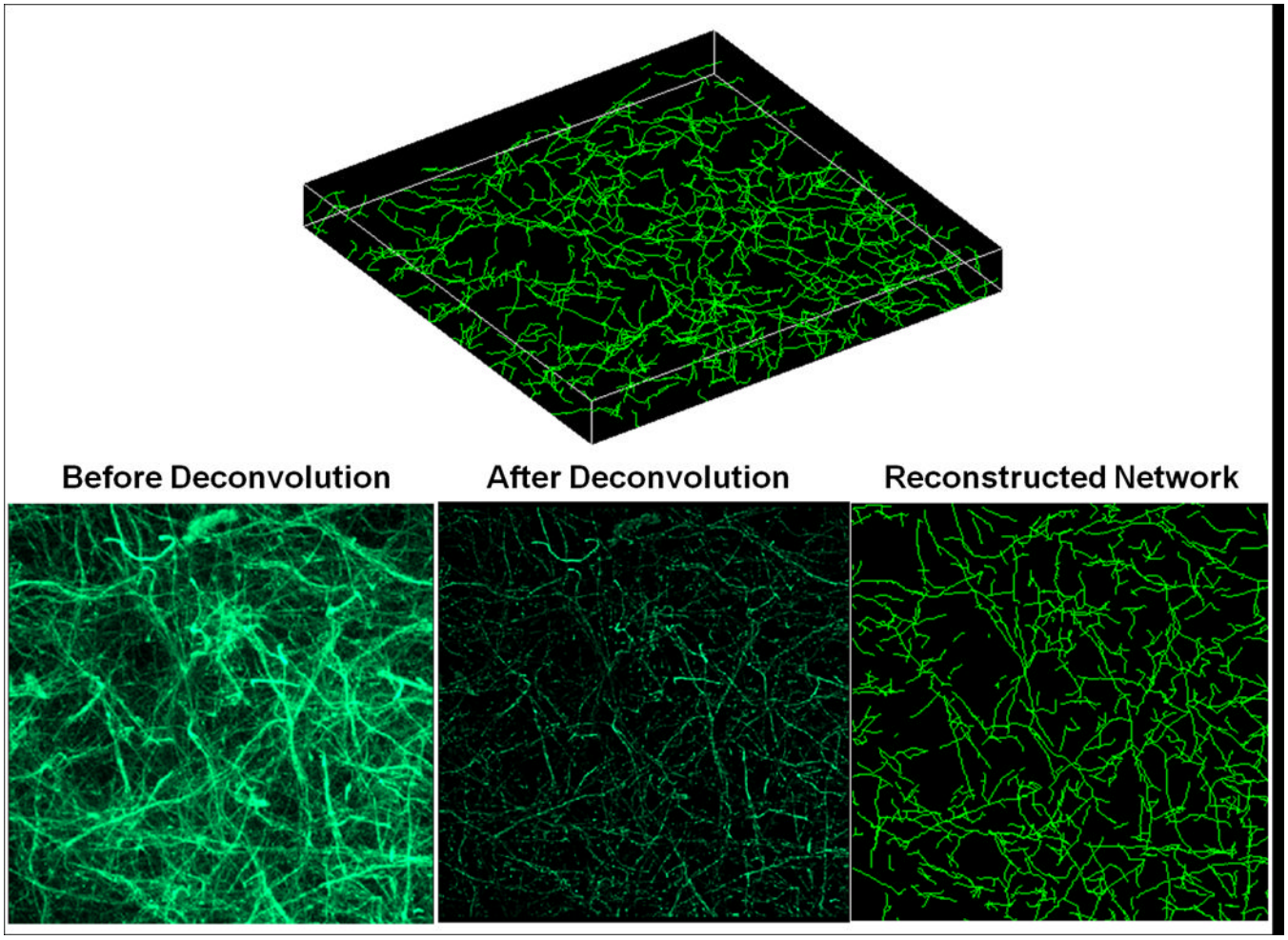

Figure 5.
Example images of a reconstructed collagen network (C in Pn). Top: Example image of the 3-D reconstructed network; final dimensions for all samples are 133μm ×133μm in-plane, with height ranging from 8 – 10μm in the z-direction. Bottom: 2-D projections of the collagen network comparing the raw collapsed z-stack image from confocal microscopy (left), the same collapsed image after deconvolution (middle), and the reconstructed network using the FIRE algorithm (right).

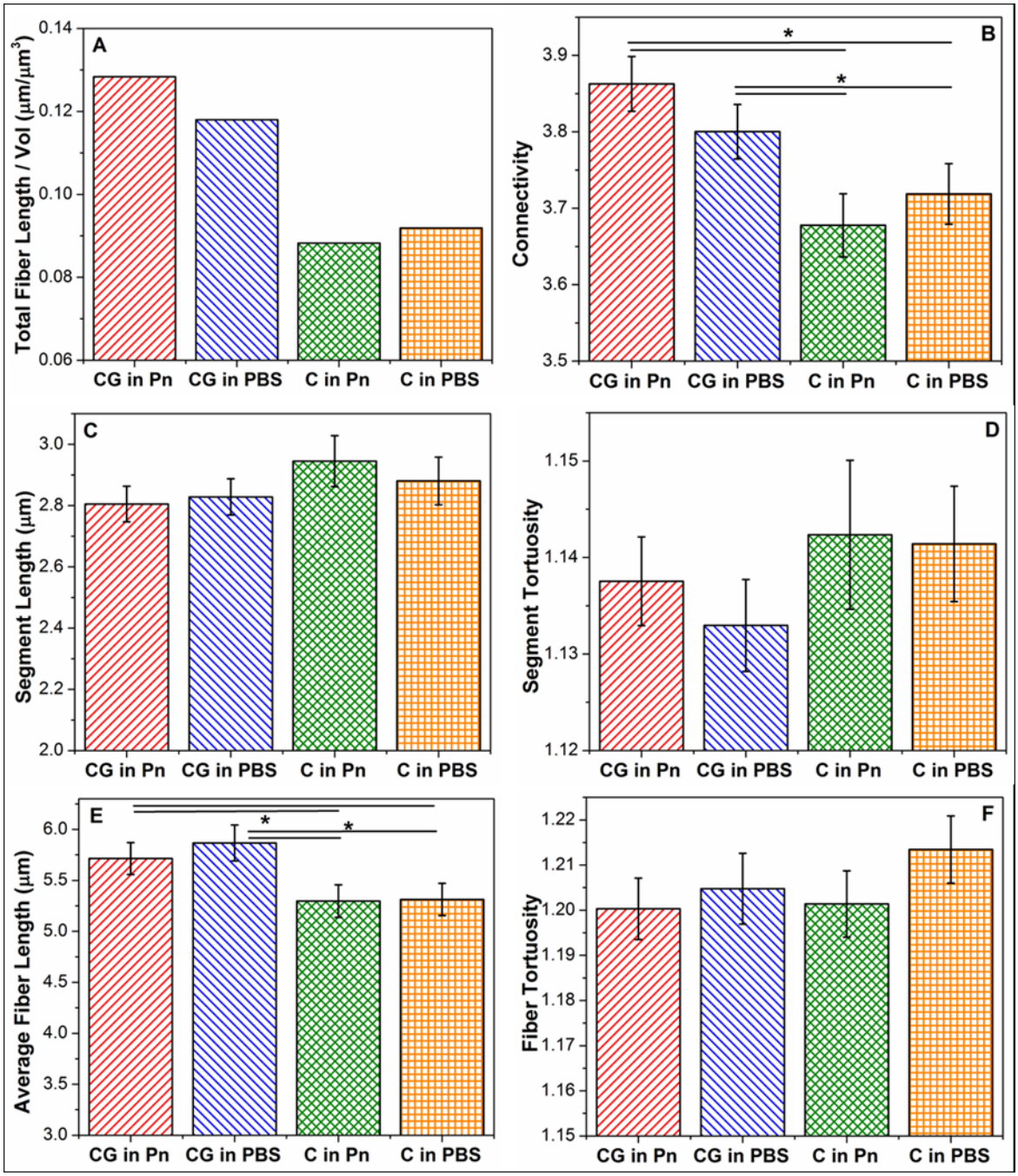

Figure 6.

Comparison of network parameters of (A) total fiber length per volume, (B), connectivity, (C) segment length, (D) segment tortuosity, (E) fiber length, and (F) fiber tortuosity between collagen networks obtained under different digestion conditions. Collagen networks obtained from co-gels (CG in PBS, CG in Pn) show high connectivities and longer average fiber lengths. Error bars represent 95% confidence intervals. * represents statistical significance at the 95% level. Note: The y-axes of these plots do not start at “0”.

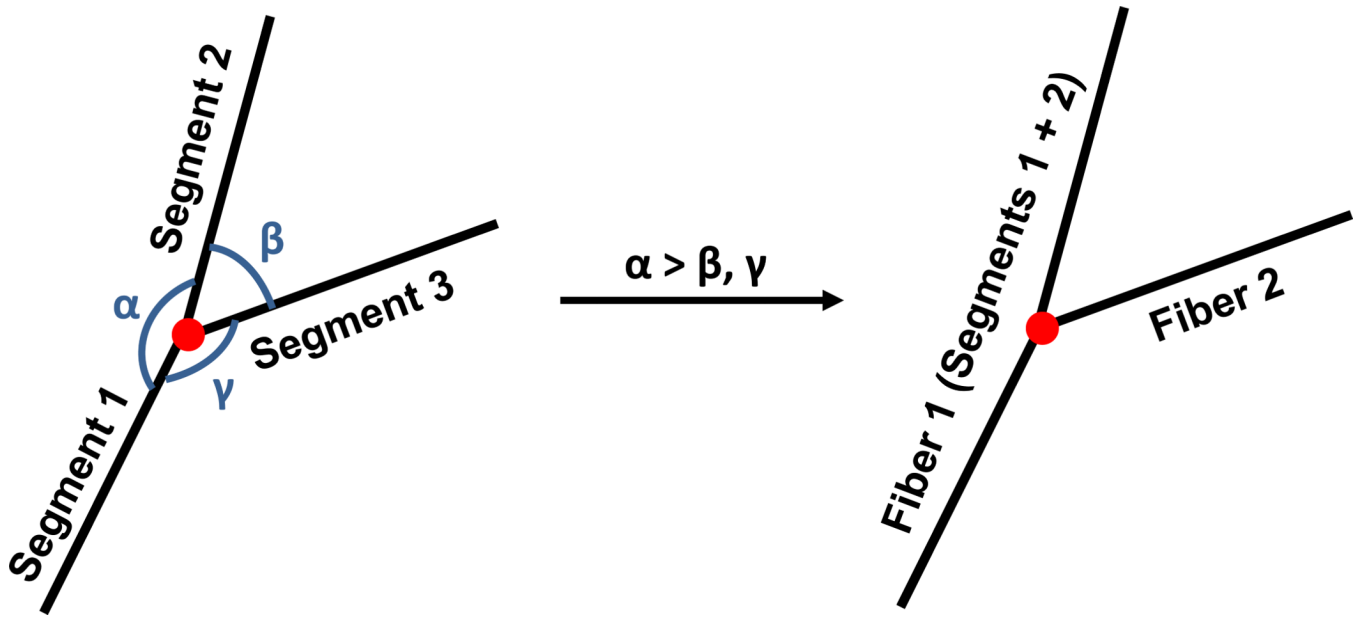

Figure 7.
Schematic representation of the definition of a segment and of a fiber in the FIRE algorithm. Each length between adjacent cross-links are defined as a segment; fibers can comprise of several segments, where segments with a similar orientation are considered part of the same fiber. α was set at 120° from sensitivity analysis.

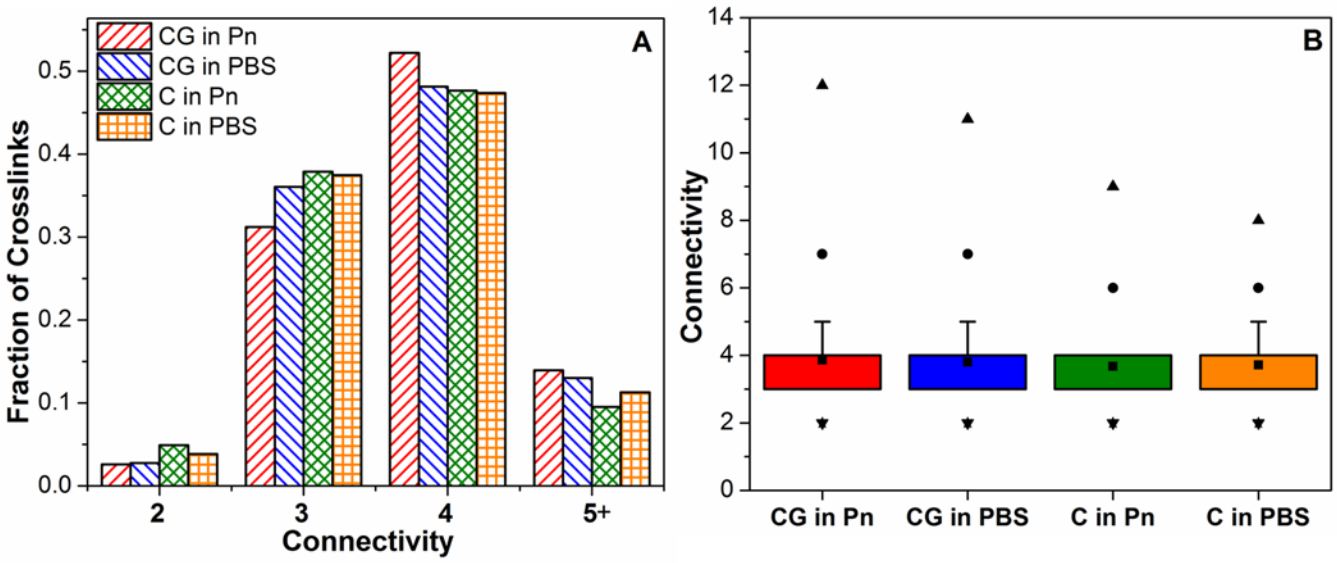

Figure 8.

Comparison of connectivity distributions in collagen networks from different casting and digestion conditions. (A) shows that >80% of cross-links contain connectivities of 3 or 4 in all samples. Box-plot in (B) shows that the collagen networks from co-gels exhibit slightly higher maximum connectivities (▲) and higher connectivities at the 99% level (●).

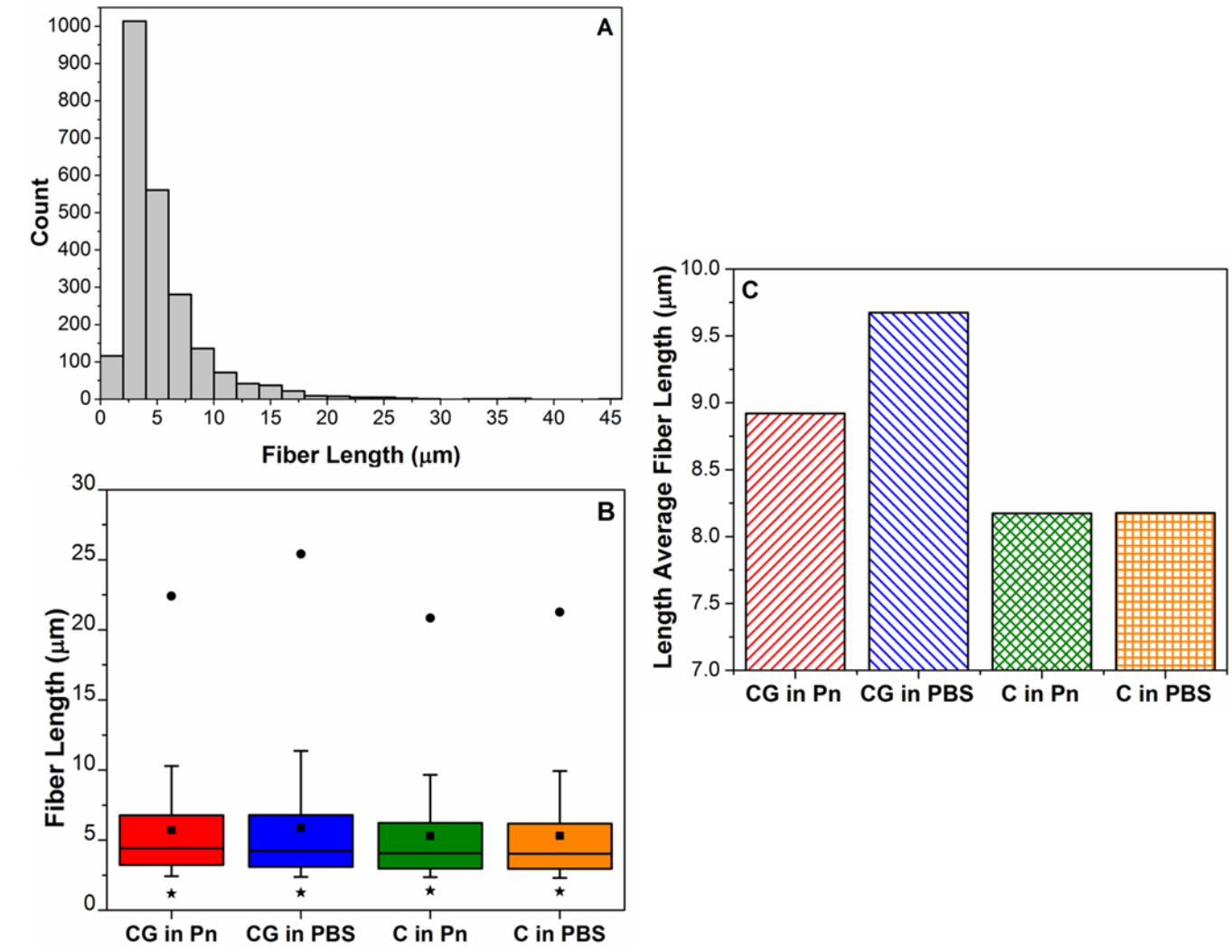

Figure 9.

Analysis of fiber lengths and their distributions in the collagen networks from different casting and digestion conditions. (A): Example of the non-normal distribution of fiber lengths in a collagen network (C in Pn). (B) Box-plot comparing fiber distributions; whiskers represent 10th to 90th percentile, ■ represents the mean, * and ● represent 1st and 99th percentile respectively. Co-gels have longer fiber lengths at 90th and 99th percentile, indicating presence of very long fibers vs. pure gels. (C) Higher length-average fiber lengths in the co-gels confirm the presence of very long fibers in the co-gels compared to the pure collagen counterparts.

Table 1

Summary of samples cast and their respective digestion treatments.

Sample	Network in Gel		Digestion Treatment	Comments
	Collagen	Fibrin		
C in PBS	•		1x PBS	Collagen control
C in Pn	•		0.02 U/ml Plasmin	Negative control for plasmin
CG in Pn	•	○	0.02 U/ml Plasmin	Resulting collagen network after fibrin digestion in co-gel
CG in PBS	•	•	PBS	Co-gel control
CG in Cs	○	•	1U/ml Collagenase	Resulting fibrin network after fibrin digestion in co-gel
F in Cs		•	1U/ml Collagenase	Negative control for collagenase
F in PBS		•	1x PBS	Fibrin control

*Positive controls were carried out by digesting collagen in collagenase and fibrin in plasmin. These gels were fully digested.

Legend:
C: Pure collagen gel
F: Pure fibrin gel
CG: Collagen-fibrin co-gel
•: network present before and after digestion
Pn: 0.02U/mL Plasmin
Cs: 1U/mL Collagenase
PBS: 1x Phosphate-Buffered Saline
○: network initially present, but digested with treatment

Table 2

Summary of results of changes in microstructure and mechanics of collagen and fibrin in collagen-fibrin co-gels, compared to their pure counterparts. Arrows represent direction of change in each characteristic for the ECM in co-gel compared to the pure gel; — means characteristic was unchanged. X for fibrin microstructure indicates these parameters were not measured.

		Collagen in Co-gel vs. Pure Collagen	Fibrin in Co-gel vs. Pure Fibrin
Microstructure	Fibril Diameter	↓	↓
	Fibril bundling	↓	N/A
	Average Fiber Length	↑	X
	Network Connectivity	↑	X
Mechanics	Strain at Failure	↑	↑
	UTS	—	—
	Tangent Modulus	↓	↓
	Transition Strain	↑	—

Table 3

pH and ionic strengths of the various gel formulations.

	pH	Ionic Strength (M)
Pure Collagen (C)	7.2	0.12
Pure Fibrin (F)	7.0	0.15
Collagen-Fibrin Co-Gel (CG)	7.2	0.16